Electro-Thermal Theory of Intermodulation Distortion in Lossy Microwave Components

Jonathan R. Wilkerson, *Student Member, IEEE*, Kevin G. Gard, *Member, IEEE*, Alexander G. Schuchinsky, *Senior Member, IEEE*, and Michael B. Steer, *Fellow, IEEE*

Abstract—An analytic formulation of dynamic electro-thermally induced nonlinearity is developed for a general resistive element, yielding a self-heating circuit model based on a fractional derivative. The model explains the 10 dB/decade slope of the intermodulation products observed in two-tone testing. Two-tone testing at 400 MHz of attenuators, microwave chip terminations, and coaxial terminations is reported with tone spacing ranging from 1 to 100 Hz.

Index Terms—Compact modeling, electrothermal, fractional calculus, fractional derivative, heat transfer, intermodulation distortion, multiphysics modeling, nonlinear computer-aided design (CAD), passive intermodulation distortion (PIM), thermal model, transient.

I. INTRODUCTION

RESISTIVE materials encounter significant self-heating when driven by high power RF signals. When the power envelope of a signal contains baseband frequency components, intermodulation distortion is generated in lossy circuit elements as their resistance varies in response to self-heating. These nonlinear effects can be dominant in high dynamic range systems and establish limits of performance. This paper presents the understanding, quantification, and modeling of the nonlinear effects that arise as a result of dynamic self-heating. A theory of electro-thermally generated intermodulation distortion for lossy materials is developed and experimentally verified using attenuators and terminations.

Passive intermodulation distortion (PIM) has been attributed to many sources including metal–oxide–metal contacts, metal–metal contacts, material defects, and dirty contacts. These sources of distortion, sometimes called "rusty bolt" effects, produce distortion signals that are at or below the noise levels of most systems [1], [2]. In contrast, electro-thermal distortion, or ET-PIM, has been shown to occur at levels

significant enough to limit the dynamic range of a system [3]. Thermal and electrical signal interaction can occur when the modulated RF signal has baseband components up to thousands of hertz when the periods of these signals are comparable to the thermal time constants of the device. These thermal transients cause time-varying resistance values resulting in close-in intermodulation components at RF. The diffusive nature of a thermal system introduces frequency dispersion and long-tail transients with nonexponential order [4]. Thermal responses have a low-pass form but with frequency domain slopes that are significantly less than the 20 dB per decade [3], [4] of a single pole response. Similar long-tail effects are seen where ever diffusive effects occur, including FETs [4]–[8]. A frequency response slope of less than 20 dB per decade can not be described in the time domain by an integer-order differential equation and instead requires a fractional calculus description.

In this paper, the understanding of thermally induced nonlinearities is developed by analyzing a general resistive component with a signal whose envelope contains instantaneous power components at baseband frequencies. To this end, heat conduction theory is reviewed for a rectangular resistive element revealing the linkage between electrical and thermal domains as well as the basis for the electro-thermal mixing process. Thermal dispersion, as it affects electrical signals, is then analyzed to account for time scaling and long tail memory effects, justifying the use of a fractional thermal model. The model enables analysis of electro-thermally induced distortion and depends on the thermo-resistance equation, thermal resistance, and thermal capacity of the material. It accurately models PIM production due to thermal processes. To physically verify the model, platinum resistors, several microwave chip terminations, and typical N-type and SMA-type terminations are characterized for thermo-resistance, thermal parameters, and RF distortion. PIM response is experimentally characterized by applying a high power two-tone signal at 400 MHz with tone spacing ranging from 1 to 100 Hz.

II. HEAT CONDUCTION AND ELECTRO-THERMAL DISTORTION

The understanding of electro-thermal distortion begins with knowledge of the coupling between electrical and thermal domains, heat conduction, and the electro-thermal mixing process. Metals exhibit a thermally based resistance that derives from the thermal dependence of electron scattering by lattice vibrations in that material [9]. This process is termed the thermo-resistance effect, and models the specific resistivity, ρ_e, (units of $\Omega \cdot m$) of a material as a function of temperature, T [10]

$$\rho_e(T) = \rho_{e0}(1 + \alpha T + \beta T^2 + \cdots). \tag{1}$$

Here, ρ_{e0} is the static resistivity constant and α and β are constants representing the temperature coefficients of resistance (TCR).

The thermo-resistance equation above couples the thermal domain to the electrical domain. Coupling from electrical to thermal domains results from dissipated electrical power, termed self-heating or joule heating. The heat generated per unit volume Q (units of $W \cdot m^{-3}$) from self heating is

$$Q = J^2 \rho_e \qquad (2)$$

where J is the current density vector in units of $A \cdot m^{-2}$. The heat produced drives the heat conduction equation

$$\nabla \cdot \left(\frac{\nabla T}{R_{th}} \right) - \rho_d c_v \frac{\partial T}{\partial t} = Q \qquad (3)$$

where c_v is the thermal capacity (units of $J \cdot K^{-1} \cdot kg^{-1}$), p_d is the density (units of $kg \cdot m^{-3}$), and the thermal resistance, (units of $K \cdot W^{-1}$) is

$$R_{th} = \frac{\Delta T}{P} = \frac{\Delta T}{I^2 R} \qquad (4)$$

where ΔT is the change in temperature with an injected thermal power P.

Thermal capacity combines the ability of a material to store heat by raising its temperature and the rate that heat is conducted to the surrounding environment. The thermal capacity at constant volume can be expressed as (units of $J \cdot K^{-1}$)

$$C_v = \left(\frac{\partial Q}{\partial T} \right)_v = T \left(\frac{\partial S}{\partial T} \right)_v = c_v \rho_d V. \qquad (5)$$

Here, S is the entropy of the system. The density, ρ_d, and volume of the material have been absorbed into the definition of the thermal capacity to represent a system of given dimensions.

The forcing function, in this case joule heating (2) with (1) can be substituted into the heat conduction equation, (3) yielding

$$\nabla \cdot \left(\frac{\nabla T}{R_{th}} \right) - C_v \frac{\partial T}{\partial t} = J^2 \rho_{e0} (1 + \alpha T + \beta T^2 + \cdots) \qquad (6)$$

which describes a nonlinear system. In practice, the first-order coefficient of the thermo-resistance equation, (1), is several orders of magnitude larger than any higher order coefficient ($\alpha \gg \beta$) in most metals, leading to its dominance in the distortion spectrum of a resistive device.

The electro-thermal process can be separated into static and dynamic components, with static and dynamic power signals P_s and P_d, respectively. The static and dynamic power signals are dissipated in the respective static and dynamic series resistance components R_s and R_d. The power dissipated over these resistance components is converted to the heat signal $Q(P_s + P_d)$ and filtered by the material thermal response. When a single RF tone is applied to a resistive element, the electro-thermal process responsible for modulating the device resistance provides a resistance with negligible dynamic variation as the thermal capacity cannot react quickly enough to the high frequency signal to significantly heat or cool the resistive material, resulting in only a step change in the static resistance due to average power dissipation. The situation changes when two or more signals are
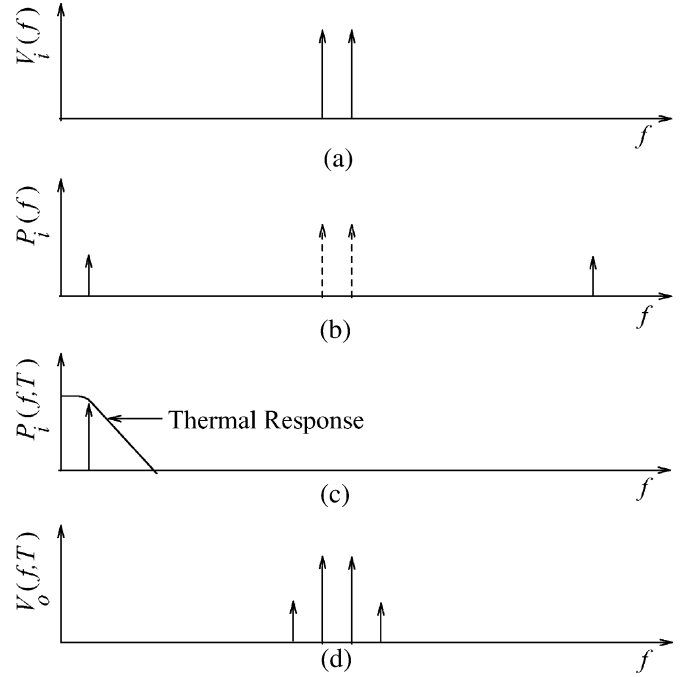

Fig. 1. Passive mixing process inherent in coupled electrical and thermal systems with: (a) input spectrum of voltages $V_i(f)$ resulting from two-tone excitation, (b) input power spectrum $P_i(f)$ resulting from a two-tone excitation, (c) component of the input power spectrum $P_i(f, T)$ at baseband able to interact with the thermal response, and (d) ouput spectrum of voltages $V_o(f, T)$ after electro-thermal mixing has occured.

applied to an electro-thermal system, as a dynamic, periodically varying resistance component becomes possible in addition to the step change in static resistance incurred from average power dissipation.

A two-tone signal $V_i(t)$, the spectrum of which is shown in Fig. 1(a), has a time-varying signal envelope. The instantaneous power of this signal varies periodically at the beat frequency of the two-tone input to the device and contains both sum and difference frequency components as shown in Fig. 1(b). If the beat frequency is within the bandwidth of the low-pass filter shown in Fig. 1(c), periodic heating and cooling of the element occurs at baseband frequencies. Consequently, the resistance of the element varies periodically. In effect this periodic oscillation creates a passive mixer producing intermodulation distortion through upconversion of the envelope frequencies at baseband to RF frequencies, resulting in the voltage output spectrum shown in Fig. 1(d).

III. FRACTIONAL TIME EVOLUTION

Thermal coupling not only leads to intermodulation distortion, but also signal dispersion due to the diffusive nature of thermal transport. Thermal dispersion can be analyzed by studying the natural response of the heat conduction equation when applied to a semi-infinite rectangular structure. In a semi-infinite rectangular structure, the heat equation becomes the 1-D differential equation

$$C_v \frac{\partial T}{\partial t} = \frac{1}{R_{th}} \left(\frac{\partial^2 T}{\partial x^2} \right) \quad (t > 0, -\infty < x < 0). \qquad (7)$$
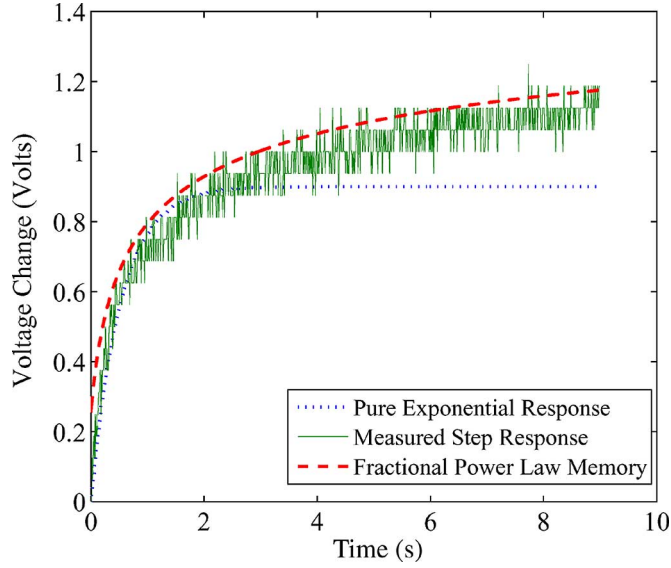
Fig. 2. Normalized power step response of resistive element exhibiting fractional power law behavior.
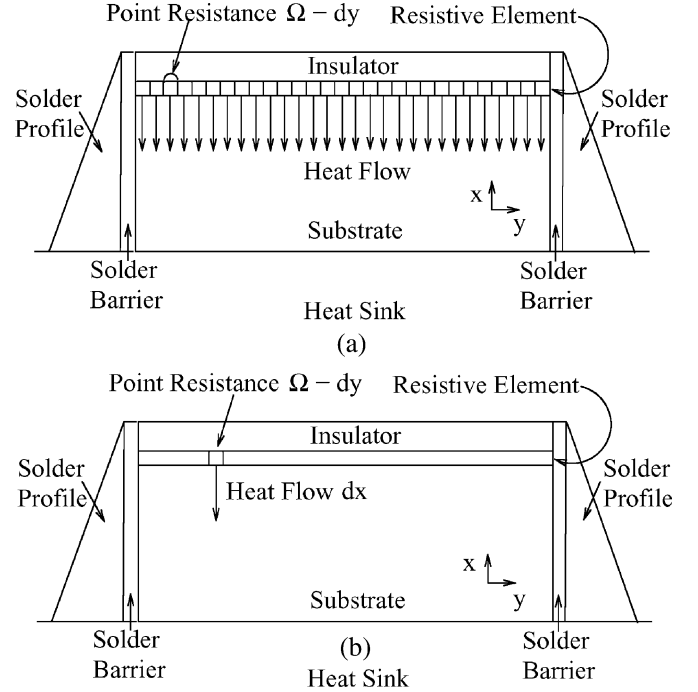

Fig. 3. Standard microwave chip termination highlighting thermodynamic environment: (a) for the entire structure and (b) for a single infinitesimal lossy element.

Insight into the nature of thermal coupled distortion products can be obtained from the solution of (7) assuming a temperature of zero at $x = -\infty$ and an initial temperature T_0 at $x = 0$. The temperature response has an error function solution [11]:

$$T(t) = T_0 \cdot \mathrm{erf}\left(\frac{x}{2\sqrt{\kappa t}}\right) \qquad (8)$$

where κ is the thermal diffusivity (units of $\mathrm{m}^2 \cdot \mathrm{s}^{-1}$) and

$$\kappa = (R_{\mathrm{th}} C_v)^{-1}. \qquad (9)$$

It is apparent from this simple solution that in diffusive situations time is effectively scaled, sometimes referred to as being dilated. The temperature at a given point in the material progresses with respect to the square root of time. Strong coupling between electrical and thermal signals due to heat conduction by electrons leads to time dilated electrical signals, where the time dilation is dependent on the strength of electrical and thermal domain coupling. The electrical signal of interest becomes dependent on a much slower thermal process, leading to inseparable time scales between electrical and thermal signals. In turn this results in a nonexponential response, sometimes called a long tail or long memory response [12]. This phenomenon is seen in Fig. 2, which shows the measured voltage step response to a current step input of a resistive element experiencing self heating. The response initially approximates an exponential, but then continues to increase with fractional power law memory.

In the literature [6], [10], [13], this behavior has been referred to as a stretched exponential response or the response of a system possessing many time constants [10]

$$T(t) = \sum_i R_i (1 - e^{-t/\tau_i}). \qquad (10)$$

This response can also be viewed as that of a filter with an infinite number of poles and zeroes [14], [15]. A new view describing the phenomena comes from the fractional calculus description of a heat conduction system. This view leads to a reduced order model for an electro-thermal system accounting for time dilation and fractional memory.

IV. FRACTIONAL HEAT CONDUCTION SYSTEM

In this section, a reduced order thermal model of a general lossy element is developed that is suitable for circuit-level models. Dynamic circuit-level models of thermal effects have used full-domain simulations and compact models [3], [10], however these models are either too computationally intensive for integration into time-stepping simulators or are not able to fully model long tail memory and dispersive effects [3]. In order to arrive at a compromise between these two simulation extremes while still maintaining the accuracy of a full-domain solution at each time point in a time-stepping circuit simulator, it is necessary to describe heat conduction from an element as though it were localized at a single spatial point. Such a description of the heat conduction equation is described here, which is the cornerstone of an accurate circuit model suitable for time-stepping simulation and an analytic derivation of electro-thermal distortion.

In any heat conduction problem, geometry and boundary conditions determine the solution of the heat transfer problem in a given medium. In order to reduce the heat conduction equation to its fractional equivalent, the heat transfer problem must be of a unidirectional nature in a semi-infinite thermal domain [16]–[18].

A chip termination can be readily modeled as a semi-infinite heat conduction system, shown in Fig. 3. A resistive element is bounded by an insulator, a thermally conductive substrate,

and a thermally conductive metal. The metal and substrate are mounted on a heat sink. The resistive element is distributed with units of ohms per square, thus the loss is distributed across the whole structure and it can be partitioned into infinitesimal elements. The thermally conductive substrate becomes large compared to the infinitesimal size of a resistive element, enabling the system to be modeled as a semi-infinite plane with parallel point heaters. Due to insulation on the top of the heater element and point heater symmetry, heat transfer can be considered to be 1-D near the actual heater element, except at the end points, which leads to negligible error for electro-thermal distortion calculations. In the electrical domain, infinitesimal resistance elements are in series, thus the combined signal with heating effects is equivalent to the lumped element resistance.

In the thermal system in Fig. 3, temperature must be finite and boundary conditions are given by

$$T(0, x) = 0 \qquad (11)$$

$$T(t, 0) = T_H(t) \qquad (12)$$

where $T_H(t)$ is the surface temperature of the resistive element, which in steady state is

$$T_H(t) = Q(t) \cdot R_{\text{th}}. \qquad (13)$$

The ambient temperature can be added to the solution through superposition, so no loss of generality is incurred by assuming an initial temperature of zero to simplify the dynamic solution. The 1-D heat equation is dependant on both time and space, giving rise to the need for separation of the domains. One method to accomplish this is the Laplace transform, which has been shown to be invertible under these boundary conditions [19]. Upon transforming the temperature,

$$\frac{1}{R_{\text{th}}} \left(\frac{\partial^2 T(s, x)}{\partial x^2} \right) - C_v s T(s, x) = 0 \qquad (14)$$

an equation dependant only on space, x is obtained, where s is the Laplace variable. Imposing boundary conditions at $x = 0$ and $x = -\infty$ (where the temperature must be zero), the solution to the ordinary differential equation (14) is

$$T(s, x) = T(s, 0) e^{x\sqrt{sC_v R_{\text{th}}}}. \qquad (15)$$

Taking the spatial derivative yields

$$\frac{\partial T(s, x)}{\partial x} = T(s, 0)\sqrt{sC_v R_{\text{th}}} e^{x\sqrt{sC_v R_{\text{th}}}}. \qquad (16)$$

Combining (15) and (16) and taking the temperature at the surface [12], [16], [20]–[22],

$$s^{-1/2}\frac{\partial T(s, 0)}{\partial x} = T(s, 0)\sqrt{C_v R_{\text{th}}}. \qquad (17)$$

The variable s in (17) represents a derivative of first order, thus $s^{1/2}$ indicates a derivative of half order. A derivative of non-integer order requires the use of fractional calculus. Here, it is defined in the Caputo sense as [12], [16], [20], [21], [23]

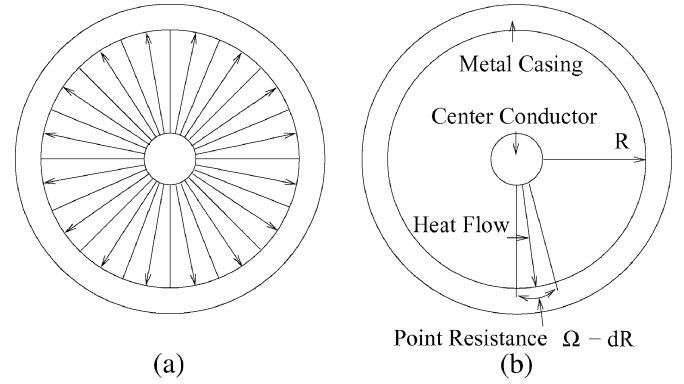$$_a^C D_t^q f(t) = \frac{1}{\Gamma(n-q)} \int_a^t \frac{f^{(n)}(\tau)}{(t-\tau)^{q+1-n}} d\tau$$

Fig. 4. Standard coaxial microwave termination highlighting the thermodynamic environment. (a) Total cross section. (b) Single infinitesimal lossy element.

$$(n - 1 \le q < n) \qquad (18)$$

where C denotes Caputo, a denotes the lower limit of the integral, q is the order of the derivative, and t is the variable the derivative is with respect to.

The path back to the time-domain solution, the inverse transform, is found through the inverse Laplace transform of the reduced order system. The fractional Laplace transform, and its inverse, are defined as [12], [16], [20], [21]

$$L\left\{_0^C D_t^q f(t); s\right\} = s^q F(s). \qquad (19)$$

Applying the inverse transform to (17) yields

$$_0 D_t^{-1/2}\frac{\partial T(t, 0)}{\partial x} = \sqrt{C_v R_{\text{th}}} T_H(t). \qquad (20)$$

Rearranging and following [12], [16], [18], [20], [21],

$$\frac{1}{R_{\text{th}}}\frac{\partial T(t, 0)}{\partial x} = \sqrt{C_v R_{\text{th}}^{-1}} \, _0 D_t^{1/2} T_H(t) \qquad (21)$$

which is the fractional form of the 1-D heat equation. Other geometries can be shown to follow similar solutions, as long as the problem is unidirectional and semi-infinite.

A standard coaxial microwave termination, shown in Fig. 4, has a cylindrical resistive disk element and has a 1-D thermal description similar to the rectangular chip construction. The fractional description is not exact in the cylindrical case [16], [18], but still maintains reasonable thermal accuracy at the point of interest [23] while accounting for the time scaling [24], [25] so important to the description of electro-thermal systems. In this case, the resistive element can still be decomposed, and the heat flow is 1-D and unidirectional radially. The outer metallic conductor acts as a heat sink, once again allowing a model of a semi-infinite plane with parallel point heaters with respect to the inner conductor.

The key to understanding the usefulness of (21) comes from realizing the nonlocality of the fractional derivative operator. This nonlocality implies that the fractional derivative of a point contains the complete knowledge of the past history of a function [12], [20]. Because of this property it is possible to use the fractional derivative as a reduced-order model where it is not
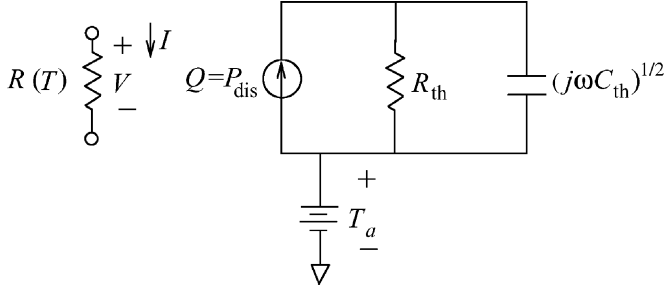
Fig. 5. Reduced order compact model for resistive element thermal node incorporating thermal dispersion.

necessary to solve the full thermal domain to obtain the temperature or heat flux at a point. This fractional-order differential equation is only dependant on the heat flux and surface temperature at a single point and accounts for the time scaling [24], [25] that occurs in the thermal domain. These aspects of the reduced-order heat conduction equation allow both the derivation of an analytic electro-thermal model and accurate prediction of electro-thermal distortion.

V. ANALYTIC MODEL OF ELECTRO-THERMAL PIM

A fractional derivative implementation of the heat conduction equation provides for the creation of a semi-compact circuit model embodying the fractional solution to the heat conduction equation. The analytic model developed in this section is suitable for time-stepping simulators, and directly leads to analytic expressions for electro-thermal distortion in lossy elements. Unlike frequency corrected compact models which are approximate over a limited bandwidth [26], fractional models link thermal and electrical domains over all frequency. Time scaling, inverse power law memory, and reduction of the solution of the heat equation from an entire structure to a single point are all accomplished in the fractional thermal circuit model.

The structure of the compact model can be determined from the solution of the application of a harmonic signal to the integer order heat equation for a semi-infinite solid. The solution to this problem is given by [11]

$$T = Ae^{-kx}\cos(\omega t - kx) \tag{22}$$
$$k = (\omega/2\kappa)^{1/2}. \tag{23}$$

It is clear that higher harmonics are attenuated as they travel into the medium. The obvious electrical analogy to represent this behavior is a low-pass filter. The low-pass filter for a thermal node is shown in Fig. 5, where the thermal capacity is now modeled by a fractional derivative based capacitor and the thermal resistance remains unchanged according to the fractional order heat conduction equation. The thermal capacitance of this model is equivalent to

$$C_{\text{th}} = C_v R_{\text{th}} \tag{24}$$

and is the thermal capacitance measured by a curve fit to the long memory transient resultant from a power step applied to the component being modeled. Heat applied to the thermal model

is just the dissipated electrical power in the modeled element. The ambient temperature is incorporated through superposition as a voltage source.

Generation of an analytic PIM expression requires reversion to a discussion of the coupling of thermal and electrical systems. The TCR equation of the device in question is the coupling equation between the two domains, and could be any order polynomial, but is generally described by the linear thermo-resistance

$$R(T) = R_0\left\{1 + \alpha\left[T(t) + T_a\right]\right\} \tag{25}$$

where R_0 is the reference resistance of the thermo-resistance equation (25) measured at 273 K on the TCR curve, T_a is the ambient temperature, and α is the first-order thermo-resistance coefficient. Instantaneous temperature is now redefined as

$$T(t) = Q(t) \cdot R_{\text{th,eq}} \tag{26}$$

where the equivalent thermal resistance is the compact fractional model equivalent resistance over frequency

$$R_{\text{th,eq}}(\jmath\omega) = \frac{R_{\text{th}}}{(1 + R_{\text{th}}\sqrt{\jmath\omega C_{\text{th}}})}. \tag{27}$$

The generated heat, (2) is thus redefined as

$$Q(t) = I(t)^2 R_0\left\{1 + \alpha\left[T(t) + T_a\right]\right\}. \tag{28}$$

The nonlinear voltage is related to the current via Ohm's Law as

$$V(t) = I(t) \cdot \left[R_0 + \alpha R_0 T_a + \alpha R_0 T(t)\right]. \tag{29}$$

Remembering that the temperature is defined in terms of the generated heat, which is itself in terms of current and temperature dependant resistance

$$\begin{aligned} T(\jmath\omega) &= Q(\jmath\omega) \cdot R_{\text{th,eq}}(\jmath\omega) \\ &= I(\jmath\omega)^2\left(R_0 + \alpha R_0 T_a + \alpha R_0 T(\jmath\omega)\right) R_{\text{th,eq}}(\jmath\omega). \end{aligned} \tag{30}$$

Current, voltage, heat, temperature, and equivalent thermal resistance dependence on frequency will be considered inherent within variables going forward, as defined in (26)–(30). Substituting this relation back into Ohm's Law, a recursion relation is obtained as follows:

$$\begin{aligned} V &= I(R_0 + \alpha R_0 T_a) + \cdots \\ &\quad I^3 \alpha R_0 R_{\text{th,eq}}(R_0 + \alpha R_0 T_a) + \cdots \\ &\quad I^5 (\alpha R_0 R_{\text{th,eq}})^2 (R_0 + \alpha R_0 T_a + \alpha R_0 T R_{\text{th,eq}}) + \cdots \end{aligned} \tag{31}$$

which can be written in closed form as

$$\begin{aligned} V &= R_0(1 + \alpha T_a)I + \\ &\quad R_0(1 + \alpha T_a)\sum_{n=1}^{\infty} I^{2n+1}(R_0 \alpha R_{\text{th,eq}})^n. \end{aligned} \tag{32}$$

Removing the dc term, the analytic representation of electro-thermal PIM is obtained (PIM_{ET}, in volts) as follows:

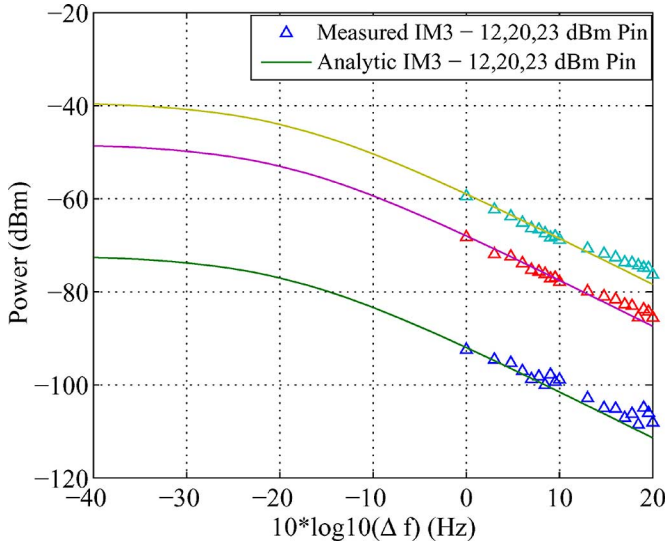$$\text{PIM}_{\text{ET}} = R_0(1 + \alpha T_a)\sum_{n=1}^{\infty} I^{2n+1}(R_0 \alpha R_{\text{th,eq}})^n. \tag{33}$$

Fig. 6. Analytic model prediction of IM3 versus tone separation overlaid on measured IM3 for platinum at 12, 20, and 23 dBm input power.
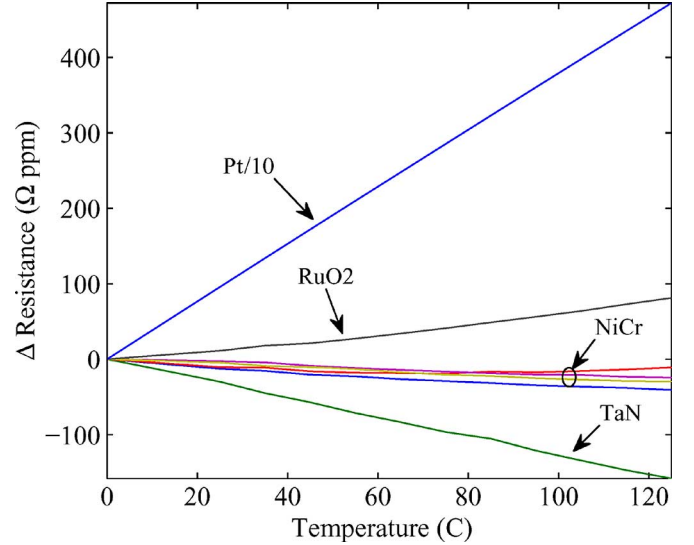

Fig. 7. TCR curves of microwave chip terminations including nichrome, platinum, tantalum nitride, and ruthenium oxide showing linear behavior of most high TCR components.

The convergence of this formula is assured through application of the ratio test

$$\lim_{n \to \infty} \left| \frac{I(\jmath\omega)^{2n+2} \left(R_0 \alpha R_{\text{th,eq}}(\jmath\omega)\right)^{n+1}}{I(\jmath\omega)^{2n+1} \left(R_0 \alpha R_{\text{th,eq}}(\jmath\omega)\right)^{n}} \right| = \left| I(\jmath\omega) \left(R_0 \alpha R_{\text{th,eq}}(\jmath\omega)\right) \right|. \tag{34}$$

Absolute convergence requires that the limit of the series be less than one, thus convergence is guaranteed for the condition

$$\left| I(\jmath\omega) \left(R_0 \alpha R_{\text{th,eq}}(\jmath\omega)\right) \right| < 1. \tag{35}$$

The analytic formulation of electro-thermal PIM includes only material and environmental parameters with the fractional derivative embedded within the equivalent thermal resistance. The analytic model includes the inverse power law memory contained within the diffusive heat conduction equation, accurately modeling electro-thermal distortion over frequency and transient long tail effects. The formula is tested by amplitude comparison against the distortion generated from applying two sinusoidal signals of equal amplitude centered at 400 MHz to a platinum device in a through configured measurement. The signal frequency spacing is swept from 1 to 100 Hz separation and is repeated at several different input power levels, as shown in Fig. 6, showing agreement with measured results.

Notably, the third-order intermodulation distortion product slope is approximately 10 dB per decade. The slope of this curve is due to the aforementioned time scaling inherent in the fractional derivative, which is native to diffusive equations. In real devices, this manifests itself as a thermal filter for IM products, where the knee is usually immeasurable in terminators due to the thermal resistance and capacity being too large for high frequency changes in thermal signals to occur. Typical 3 dB points for these devices are below 0.01 Hz. Distortion products are generated when the envelope of the signal falls within the thermal filter, which is shaped by the long memory and upconverted to microwave frequencies.

VI. MEASUREMENT AND DISCUSSION

Accurate modeling of thermal induced distortion requires knowledge of the material thermo-resistance equation parameters, thermal capacity, and thermal resistance, while validation of the model requires two-tone distortion characterization of the device. Three separate measurements are required to determine and validate all of the necessary model parameters. Device TCR can be found by characterizing resistance change over temperature. Thermal capacity and resistance are obtained through the application of a power step and subsequent measurement of the ensuing thermal transient. Two-tone characterization of electro-thermal distortion can be accomplished through a tone spacing sweep, which provides model validation and inverse extraction of modeling parameters. Each of the measurements necessary for model identification and validation are detailed in the subsequent TCR, thermal transient, and two-tone IM characterization subsections.

A. TCR Characterization

The thermo-resistance effect was characterized using a thermal chamber, high accuracy current sources, and voltage meters to measure the change in resistance over the operational temperature of the device under test. Measured thermo-resistance curves are shown in Fig. 7 for several terminations composed of nichrome, tantalum nitride, and ruthenium oxide as well as a platinum element.

The platinum element is thermally the most linear and has the highest linear TCR. Distortion levels for this device are also the highest per unit power of all devices examined. Several of the terminations exhibit thermo-resistance curves which are strongly nonlinear over the operational temperature range, yet still possess TCR that are relatively small in magnitude. These elements produce distortion levels immeasurable in the system. Distortion is orders of magnitude lower than that of the linear thermo-resistance devices even though they exhibit much more nonlinear thermo-resistances. Clearly the slope of

the thermo-resistance over the operation range is the dominant effect on device distortion. For devices with strongly nonlinear thermo-resistance, the temperature dependence on distortion co-efficients must be considered for accurate modeling.

B. Thermal Transient Characterization

Several methods can be used to determine thermal resistance and capacity, including the three omega method [27], thermal cameras, and current step tests [28]. As distortion will depend on the entire systems heat sinking condition, a current step applied to the device in its environment of interest provides an accurate portrayal of device operational characteristics. By measuring voltage response and converting to power, the power step response can be fit as if it were a simple low-pass filter response, given by [28]

$$P(t) = P_0(1 - e^{-t/R_{th}C_{th}}). \quad (36)$$

Thermal resistance is then the difference in the final value of resistance for a given power step minus the ambient resistance, normalized to the power. Thermal capacity is given by fitting the transient response of the power step and employing the measured value of thermal resistance. Care must be taken in performing such a fit, as devices exhibiting significant electro-thermal distortion will have long thermal memory. Fitting the initial exponential response of the long tail effect and the end value of the transient, combined with the corresponding thermal resistance provides reasonably accurate results with minimal fitting effort. Thermal cameras can be used in the same manner, with a temperature step and curve fit of the response.

C. Two-Tone PIM Characterization

Sweeping the spacing of a two-tone signal is effective in characterizing thermally induced distortion in RF systems, as it produces a sinusoidal thermal signal within the thermal response bandwidth. Low PIM components in the measurement system must be used to guarantee measurement integrity. Commercially available spectrum analyzers are limited to less than 85 dB dynamic range, and the vector signal analyzer used in this test was limited to approximately 75 dB. In order to circumvent this limitation at low tone spacing where filtering is not an option, an active cancellation system was built to allow accurate, high dynamic range measurements of at least 95 dB [29].

Devices measured include chip terminations composed of tantalum nitride, platinum, and nichrome. Further measurements of typical lab terminations in N-type and SMA-type configurations were also conducted. Device TCR ranged from 150 to 3850 ppm. Tantulum nitride, platinum, and coaxial laboratory terminations all produced measurable distortion in direct agreement with the fractional electro-thermal model. Power levels during testing were at one quarter or less of rated device power for N-type and SMA type terminations. Nichrome terminations were TCR panned, putting their distortion at levels below measurement capability. Using measured values for thermal resistance, capacity, and device TCR, measurement results for IM3 are compared to the electro-thermal analytic model in Fig. 8. Fig. 8 compares the analytic electro-thermal model with measured results of distortion generated from
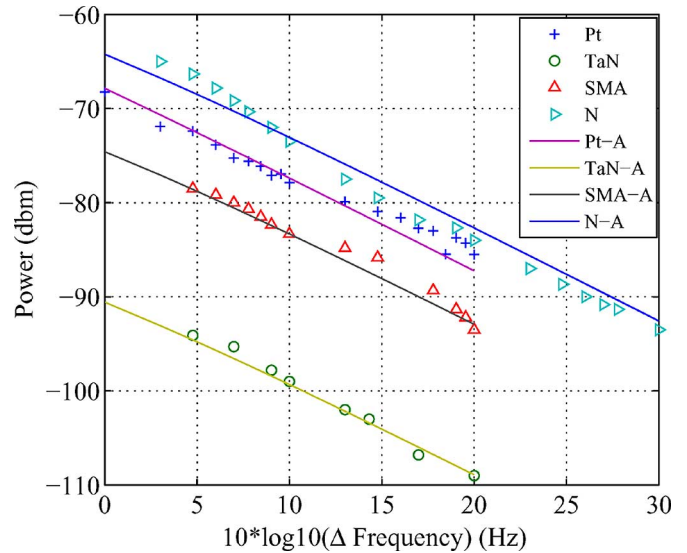

Fig. 8. Analytic prediction and measured distortion for platinum, tantalum nitride, SMA type terminator, and N type terminator for two tone spacing swept excitation at 20, 30, 27, and 25 dBm input power per tone, respectively.

applying two sinusoidal signals of equal amplitude centered at 400 MHz to the various devices in a through configured measurement where the signal frequency spacing is swept from 1 Hz to 100 Hz separation. Measurement and model results coincide for all measurable materials for both cylindrical and planar semi-infinite geometries. Agreement between model and measurement demonstrates the necessity of a semi-derivative formulation for heat transfer to account for thermal time scaling in the electrical domain.

The intermodulation distortion magnitude in Fig. 8 is dependant on tone spacing and consequently signal bandwidth for a modulated signal. Fortunately, several other factors can reduce distortion levels to a bare minimum regardless of the signal applied. From the analytic model presented and matching measurement data, two factors become obvious for minimum electro-thermal PIM design when signal bandwidth cannot be controlled. First, and most important, is the device TCR, which must be reduced to a minimum over the operational range. Operational temperature must be kept away from any sharp sloped areas of the thermo-resistance curve. This can be accomplished through material manufacture methods, careful design of power dropped over resistive elements, or heat sinking to guarantee a maximum dynamic temperature rise over operational power. Thermal resistance and thermal capacity are material and size dependant parameters that control the bandwidth of the thermal filter. As the knee of the thermal filter increases in frequency, distortion levels due to electro-thermal distortion will increase toward their maximum level. Generally, increasing the size of the device will decrease distortion by increasing overall thermal capacity and reducing system thermal resistance. Choice of materials should focus on highest thermal conductivity for minimum distortion.

VII. CONCLUSION

In a thermally coupled RF electrical system, electro-thermal passive distortion products exist at levels prohibitive to high

power system performance. For applications requiring high linearity, prediction of these distortion products is crucial for proper design. A new analytic model based on the reduction of the heat equation to a fractional order differential equation has been presented for determining this distortion based only on material parameters and measurement of device TCR characteristics. Model validation was accomplished through measurement of several microwave chip terminations and standard lab SMA and N type terminations. All terminations were excited by a two-tone signal with swept tone spacing for distortion measurements. Analytic formula and measurement data matched with very good agreement, demonstrating the necessity of a fractional formulation of heat conduction for accurate electro-thermal distortion prediction. Device TCR was found to be the dominant factor in electro-thermal distortion generation, and can lead to temperature-dependant distortion coefficients. Thermal filter characteristics should also be minimized through limiting change in device temperature through proper heat sinking, material choice, and device sizing.

REFERENCES

[1] C. Vicente and H. L. Hartnagel, "Passive-intermodulation analysis between rough rectangular waveguide flanges," *IEEE Trans. Microw. Theory Tech.*, vol. 53, no. 8, pp. 2515–2525, Aug. 2005.

[2] H. Huan and F. Wen-Bin, "On passive intermodulation at microwave frequencies," in *Proc. Asia–Pacific Environ. Electromagn. Conf.*, Nov. 2003, pp. 422–425.

[3] J. R. Wilkerson, K. G. Gard, and M. B. Steer, "Electro-thermal passive intermodulation distortion in microwave attenuators," in *Proc. 36th Eur. Microw. Conf.*, Sept. 2006, pp. 157–160.

[4] A. E. Parker and J. G. Rathmell, "Self-heating process in microwave transistors," in *URSI Commission C Appl. Radio Sci. Workshop*, P. Wilkinson, Ed., Hobart, Australia, 2004, pp. 1–8. [Online]. Available: http://www.ips.gov.au/IPSHosted/NCRS/wars/wars-2004/index.htm

[5] J. S. Brodsky, R. M. Fox, D. T. Zweidinger, and S. Veeraraghavan, "A physics-based, dynamic thermal impedance model for SOI MOSFET's," *IEEE Trans. Electron Devices*, vol. 44, no. 6, pp. 957–963, Jun. 1997.

[6] A. E. Parker and J. G. Rathmell, "Broad-band characterization of FET self-heating," *IEEE Trans. Microw. Theory Tech.*, vol. 53, no. 7, pp. 2424–2429, Jul. 2005.

[7] K. Lu, P. M. McIntosh, C. M. Snowden, and R. D. Pollard, "Low-frequency dispersion and its influence on the intermodulation performance of AlGaAs/GaAs HBTs," in *IEEE MTT-S Int. Microw. Symp. Dig.*, 1996, pp. 1373–1376.

[8] J. Brinkhoff and A. E. Parker, "Effect of baseband impedance on FET intermodulation," *IEEE Trans. Microw. Theory Tech.*, vol. 51, no. 3, pp. 1045–1051, Mar. 2003.

[9] G. T. Meaden, *Electrical Resistance of Metals*. New York: Plenum, 1965.

[10] T. Bechtold, E. Rudnyi, and J. Korvink, "Dynamic electro-thermal simulation of microsystems—A review," *Micromech. Microeng.*, vol. 15, no. 11, pp. R17–R31, Oct. 2005.

[11] H. S. Carslaw and J. C. Jaeger, *Conduction of Heat in Solids*. New York: Oxford Univ. Press, 1959.

[12] B. J. West, M. Bologna, and P. Grigolini, *Physics of Fractal Operators*. New York: Springer, 2003.

[13] G. Meneghesso, G. Verzellesi, R. Pierobon, F. Rampazzo, A. Chini, U. K. Mishra, C. Canali, and E. Zanoni, "Surface-related drain current dispersion effects in AlGaN-GaN HEMTs," *IEEE Trans. Electron Devices*, vol. 51, no. 10, pp. 1554–1561, Oct. 2004.

[14] G. C. Temes and J. W. LaPatra, *Introduction to Circuit Synthesis and Design*. New York: McGraw-Hill, 1977.

[15] K. Kundert, "Modeling dielectric absorption in capacitors," 1982. [Online]. Available: http://www.designers-guide.org/

[16] K. B. Oldham and J. Spanier, *The Fractional Calculus*. New York: Academic, 1974.

[17] V. V. Kulish and J. L. Lage, "Fractional-diffusion solutions for transient local temperature and heat flux," *Trans. Amer. Soc. Mech. Eng.*, vol. 122, pp. 372–376, May 2000.

[18] K. B. Oldham and J. Spanier, "A general solution of the diffusion equation for semiinfinite geometries," *Math. Anal. Appl.*, vol. 39, pp. 655–669, 1972.

[19] H. S. Carslaw and J. C. Jaeger, *Operational Methods in Applied Mathematics*. New York: Dover, 1963.

[20] I. Podlubny, *Fractional Differential Equations*. New York: Academic, 1999.

[21] K. S. Miller and B. Ross, *Fractional Calculus and Fractional Differential Equations*. New York: Wiley, 1993.

[22] L. P. Kholpanov and S. E. Zakiev, "Fractional integro-differential analysis of heat and mass transfer," *Eng. Phys. Thermophys.*, vol. 78, no. 1, pp. 33–46, 2005.

[23] O. P. Agrawal, "Application of fractional derivatives in thermal analysis of disk brakes," *Nonlinear Dynam.*, vol. 38, pp. 191–206, 2004.

[24] C. Ma and Y. Hori, "Geometric interpretation of discrete fractional order controllers based on sampling time scaling property and experimental verification of fractional $1/S^\alpha$ system's robustness," in *Proc. Amer. Soc. Mech. Eng. Tech. Design Eng. Conf.*, Dec. 2007, pp. 1–6.

[25] C. Ma and Y. Hori, "The time-scaled trapeziodal integration rule for discrete fractional order controllers," *Nonlinear Dynam.*, vol. 38, pp. 171–180, 2004.

[26] T. Poinot and J. C. Trigeassou, "A method for modeling and simulation of fractional systems," *Signal Process.*, vol. 83, pp. 2319–2333, 2003.

[27] D. G. Cahill, "Thermal conductivity measurement from 30 to 750 K: The 3ω method," *Rev. Sci. Instrum.*, vol. 61, no. 2, pp. 802–808, Feb. 1999.

[28] Z. Szepessy and I. Zoltan, "Thermal dynamic model of precision wire-wound resistors," *IEEE Trans. Instrum. Meas.*, vol. 51, no. 5, pp. 930–934, Oct. 2002.

[29] J. R. Wilkerson, K. G. Gard, and M. B. Steer, "Wideband high dynamic range distortion measurement," in *IEEE Radio Wireless Symp.*, Orlando, FL, Jan. 2008, pp. 415–418.
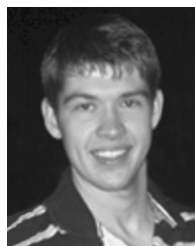
Jonathan R. Wilkerson (S'08) was born in Greenville, NC. He received the B.S. degree in electrical engineering and computer engineering and M.S. degree in electrical engineering from North Carolina State University, Raleigh, in 2005 and 2006, respectively, and is currently working toward the Ph.D. degree at North Carolina State University.

He is currently a Graduate Research Assistant with the ERL Laboratory, Electrical and Computer Engineering Department, North Carolina State University.

Kevin G. Gard (S'92–M'95) received the B.S. and M.S. degrees in electrical engineering from North Carolina State University, Raleigh, in 1994 and 1995, respectively, and the Ph.D. degree in electrical engineering from the University of California at San Diego, La Jolla, in 2003.

He is currently the William J. Pratt Assistant Professor with the Electrical and Computer Engineering Department, North Carolina State University. From 1996 to 2003, he was with Qualcomm Inc., San Diego, CA, where he was a Staff Engineer and Manager responsible for the design and development of RF integrated circuits (RFICs) for code-division multiple-access (CDMA) wireless products. He has designed SiGe BiCMOS, Si BiCMOS, and GaAs metal–semiconductor field-effect transistor (MESFET) integrated circuits for cellular and personal communication systems (PCSs) CDMA, WCDMA, and AMPS transmitter applications. His research interests are in the areas of integrated circuit design for wireless applications and analysis of nonlinear microwave circuits with digitally modulated signals. He has authored or coauthored over 60 papers related to RF/analog integrated circuit design and analysis of nonlinear circuits.

Dr. Gard is a member of the IEEE Microwave Theory and Techniques Society (IEEE MTT-S) and IEEE Solid-State Circuits Society. He is a member of Eta Kappa Nu and Tau Beta Pi. In 2007, He was secretary of the IEEE MTT-S Administrative Committee (AdCom) in 2007.

Alexander G. Schuchinsky (M'97–SM'05) received the M.Sc. degree in radiophysics from Rostov State University, Rostov-on-Don, Russia, in 1973, the Ph.D. degree in radiophysics from the Leningrad Electrotechnical Institute, Leningrad, Russia, in 1983, respectively, and the title of Senior Research Scientist in 1988.

From 1973 to 1994, he was with the Microwave Electrodynamics Laboratory, Rostov State University, where he was the Leading Scientist. From 1994 to 2002, he was with Deltec-Telesystems New Zealand. Since 2002, he has been a Reader with the School of Electronics, Electrical Engineering and Computer Science, Queen's University Belfast, Belfast, U.K. He has authored or coauthored over 130 papers in major Journal and Conference Proceedings. He is a member of the Editorial Board of *Metamaterials*. He holds three U.S. patents. His current research interests include numerical–analytical and physics-based modeling techniques, microwave and optical phenomena in complex media, metamaterials, periodic structures with linear and nonlinear inclusions, electromagnetic characterization and measurements of materials, and microwave applications of novel materials.

Dr. Schuchinsky is a member of the European Physical Society. He served as a chair of the Steering Committee of the International Congress on Advanced Electromagnetic Materials in Microwaves and Optics (Metamaterials'2007).

Michael B. Steer (S'76–M'82–SM'90–F'99) received the B.E. and Ph.D. degrees in electrical engineering from the University of Queensland, Brisbane, Australia, in 1976 and 1983, respectively.

He is currently the Lampe Professor of Electrical and Computer Engineering with North Carolina State University, Raleigh. In 1999 and 2000, he was Professor with the School of Electronic and Electrical Engineering , The University of Leeds, where he held the Chair in Microwave and Millimeter-Wave Electronics. He was also Director of the Institute of Microwaves and Photonics, The University of Leeds. He has authored 400 publications on topics related to RF, microwave and millimeter-wave systems, high-speed digital design, and RF and microwave design methodology and circuit simulation. He has authored *Microwave and RF Design: A Systems Approach* (SciTech, 2008). He coauthored *Foundations of Interconnect and Microstrip Design* (Wiley, 2000) and *Multifunctional Adaptive Microwave Circuits and Systems* (SciTech, 2009).

Prof. Steer is active in the IEEE Microwave Theory and Technique Society (IEEE MTT-S). In 1997, he was secretary of the IEEE MTT-S, and from 1998 to 2000, he was an elected member of the IEEE MTT-S Administrative Committee (AdCom). He was the Editor-in-Chief of the IEEE TRANSACTIONS ON MICROWAVE THEORY AND TECHNIQUES (2003–2006) He was a 1987 Presidential Young Investigator (USA). In 1994 and 1996, he was the recipient of the Bronze Medallion presented by the U.S. Army Research Office for Outstanding Scientific Accomplishment. He was also the recipient of the Alcoa Foundation Distinguished Research Award presented by North Carolina State University in 2003.